ON THE EFFECTIVENESS OF AUTOMATED CONFIGURATION IN ABSTRACT ARGUMENTATION REASONING

Federico Cerutti[†] · Mauro Vallati[*] · Massimiliano Giacomin[+]

xv · ix · mmxvi

[†]Cardiff University · [*] University of Huddersfield · [+]Università degli Studi di Brescia

Definition

An *argumentation framework* (AF) is a pair $\Gamma = \langle \mathcal{A}, \mathcal{R} \rangle$ where $\mathcal{A}$ is a set of arguments and $\mathcal{R} \subseteq \mathcal{A} \times \mathcal{A}$. We say that $\mathbf{b}$ *attacks* $\mathbf{a}$, or $\mathbf{b} \to \mathbf{a}$, iff $\langle \mathbf{b}, \mathbf{a} \rangle \in \mathcal{R}$.

Given an AF $\Gamma = \langle \mathcal{A}, \mathcal{R} \rangle$:

- a set S $\subseteq \mathcal{A}$ is a *conflict–free* set of Γ if $\nexists\, \mathbf{a}, \mathbf{b} \in$ S s.t. $\mathbf{a} \to \mathbf{b}$;
- an argument $\mathbf{a} \in \mathcal{A}$ is *acceptable* with respect to a set S $\subseteq \mathcal{A}$ of Γ if $\forall \mathbf{b} \in \mathcal{A}$ s.t. $\mathbf{b} \to \mathbf{a}$, $\exists\, \mathbf{c} \in$ S s.t. $\mathbf{c} \to \mathbf{b}$;
- a set S $\subseteq \mathcal{A}$ is an *admissible set* of Γ if S is a conflict–free set of Γ and every element of S is acceptable with respect to S of Γ;
- a set S $\subseteq \mathcal{A}$ is a *preferred extension* of Γ iff S is a maximal (w.r.t. set inclusion) admissible set of Γ.

Computational Models of Argument
S. Parsons et al. (Eds.)
IOS Press, 2014

doi:10.3233/978-1-61499-436-7-455

ArgSemSAT: Solving Argumentation Problems Using SAT

Federico CERUTTI[a,1], Massimiliano GIACOMIN[b], and Mauro VALLATI[c]
[a] *Department of Computing Science, King's College, University of Aberdeen, UK*
[b] *Department of Information Engineering, University of Brescia, Italy*
[c] *School of Computing and Engineering, University of Huddersfield, UK*

Abstract. In this paper we describe the system ArgSemSAT which includes algorithms which we proved to overcome current state-of-the-art performances in enumerating preferred extensions.

Keywords. argumentation, argumentation semantics, extensions enumeration

1. Introduction

Dung's theory of abstract argumentation frameworks provides a fundamental reference in computational argumentation in virtue of its simplicity, generality, and ability to capture a variety of more specific approaches as special cases. An abstract argumentation framework (AF) consists of a set of arguments and an *attack* relation between them. The concept of *extension* plays a key role in this simple setting, where an *extension* is intuitively a set of arguments which can "survive the conflict together". Different notions of extensions and of the requirements they should satisfy correspond to alternative *argumentation semantics*.

The main computational problems in abstract argumentation are related to extensions and can be partitioned into two classes: *decision* problems and *construction* problems. In particular, *extension enumeration* requires to construct *all* extensions prescribed for a given AF: its solution provides complete information concerning the justification status of arguments and subsumes the solutions to the other problems. On the practical side, few results are available on the development of efficient algorithms for abstract argumentation and their empirical assessment. In [1, 2] SAT-based approaches have been proposed to solve the extension enumeration problem for preferred semantics.

2. Overview of ArgSemSAT

ArgSemSAT is a collection of algorithms[2] mainly developed for enumerating preferred extensions which proved [1, 2] to be more efficient, in terms of time performance, than current state-of-the-art approaches.

[1] Corresponding Author
[2] http://tiny.cc/argsemsat

Parameter	Domain	Default
SOLVER-ExtEnc	{001111, 010101, 010111, 011101, 011111, 101010, 101011, 101110, 101111, 110011, 110101, 110111, 111011, 111100, 111101, 111110, 111111}	101010
GLUCOSE-gc-frac	[0.0, 500.0]	0.2
GLUCOSE-rnd-freq	[0.0, 1.0]	[0.0
GLUCOSE-cla-decay	[0.0, 1.0]	0.999
GLUCOSE-max-var-decay	[0.0, 1.0]	0.95
GLUCOSE-var-decay	[0.0, 1.0]	0.8
GLUCOSE-phase-saving	0,1,2	2
GLUCOSE-ccmin-mode	0,1,2	2
GLUCOSE-K	[0.0, 1.0]	0.8
GLUCOSE-R	[1.0, 5.0]	1.4
GLUCOSE-szTrailQueue	[10,10000] (int)	5000
GLUCOSE-szLBDQueue	[10,10000] (int)	50
GLUCOSE-simp-gc-frac	[0.0, 5000.0]	0.5
GLUCOSE-sub-lim	[-1,10000] (int)	20
GLUCOSE-cl-lim	[-1,10000] (int)	1000
GLUCOSE-grow	[-10000,10000] (int)	0
GLUCOSE-incReduceDB	[0,10000] (int)	300
GLUCOSE-firstReduceDB	[0,10000] (int)	2000
GLUCOSE-specialIncReduceDB	[0,10000] (int)	1000
GLUCOSE-minLBDFrozenClause	[0,10000] (int)	30

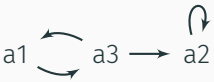

arg(a1).
arg(a2).
arg(a3).
att(a1,a3).
att(a2,a2).
att(a3,a1).
att(a3,a2).

arg(a2).
arg(a3).
arg(a1).
att(a2,a2).
att(a3,a2).
att(a3,a1).
att(a1,a3).

List of arguments ordered according to the number of received attacks and, subsequently, the number of outgoing attacks; and the list of attacks ordered prioritising self-attacks and, subsequently, the number of outgoing attacks

ONLINE CONFIGURATION

Order arguments/attacks according to:

1. The number of attacks received;
2. The number of attacks to other arguments;
3. The presence of self-attacks;
4. The difference between the number of received attacks and the number of attacks to other arguments;
5. Being an argument in a mutual attack.

+ arguments can be listed following a direct or inverse order

Ordering of arguments and attacks are independent

Parameter	Domain	Default
args_ingoingFirst	[-1.0,1.0]	0
args_outgoingFirst	[-1.0,1.0]	0.2
args_autoFirst	[-1.0,1.0]	-1
args_eachOther	[-1.0,1.0]	-1
args_differenceFirst	[-1.0,1.0]	-1
atts_ingoingFirst	[-1.0,1.0]	0
atts_outgoingFirst	[-1.0,1.0]	0
atts_autoFirst	[-1.0,1.0]	0.2
atts_eachOther	[-1.0,1.0]	0
atts_differenceFirst	[-1.0,1.0]	0
atts_orders	{0,1,2,3,4}	0

0 Same ordering applied to the first argument of the attack pair
1 Same ordering applied to the second argument of the attack pair
2 Inverse ordering applied to the first argument of the attack pair
3 Inverse ordering applied to the second argument of the attack pair
4 Attack-specific ordering

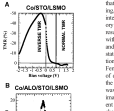

Fig. 3. Bias dependence of the TMR ratio in **(A)** Co/STO/LSMO and **(B)** Co/ALO/STO/LSMO tunnel junctions.

level of LSMO is situated above the Fermi level of Co and a maximum of inverse TMR is expected when the Fermi level of LSMO is approximately at the maximum of the spin ↓ DOS of Co. This is consistent with the maximum of inverse TMR observed at ~ −0.4 V for Co/STO/LSMO junctions (Fig. 3A). For a positive bias, the TMR is expected to change sign and become normal above 1 V when the Fermi level of LSMO goes down into the energy range of the majority spin d-band of Co. This is also observed in Fig. 3A.

For ALO and ALO/STO barriers, a predominant tunneling of s-character electrons (see arrow in Fig. 2B) is the usual explanation of the positive polarization (6–9). The rapid drop with bias (Fig. 3B) is similar to what has been observed in most junctions with ALO barriers, and completely different from what is obtained when the tunneling is predominantly by d-character electrons (Fig. 3A). The origin of this rapid decrease of the TMR at relatively small bias has never been clearly explained. This is roughly consistent with the energy dependence of the DOS induced by sp-d bonding effects on the first atomic layer of ALO in the calculation of Nguyen-Mahn *et al.* (*8*) for the Co-ALO interface. But Zhang *et al.* (*13*) have also shown that a large part of the TMR drop can be attributed to the excitation of spin waves.

The experiments reported here and in several recent publications (*1*, *4*) demonstrate the important role of the electronic structure of the metal-oxide interface in determining the spin polarization of the tunneling electrons. The negative polarization for the Co-STO interface has been ascribed to d-d bonding effects between Al and Ti (*4*). This interpretation is similar to that proposed to explain, in terms of sp-d bonding, the positive polarization at the Co-ALO interface (*8*). However, there is no general theory predicting the trend of the experimental results for Co—that is, a negative polarization with oxides of d elements (STO, CLO, Ta_2O_5) and a positive one when there are only s and p states (ALO). It is likely that the spin polarization should also depend on the position of the Fermi level with respect to the electronic levels of each character above and below the gap of the insulator. In addition, as an evanescent wave in an insulator is a Bloch wave with an imaginary wave vector, one can expect different decay lengths for Bloch waves of different character. This means that the final polarization could also depend on the thickness of the barrier, as illustrated by the calculations of Maclaren *et al.* for Fe/ZnSe/Fe junctions (*14*).

The influence of the barrier on the spin polarization opens new ways to shape and optimize the TMR. Interesting bias dependences can be obtained with barriers selecting the d electrons and probing the fine structure of the d-DOS, as in Fig. 3A. The DOS of a d-band can also be easily tailored by alloying (for example, by introduction of virtual bound states) to produce specific bias dependencies. Although here we concentrated on the problem of the spin polarization of the Co electrode and regarded the strongly spin-polarized LSMO only as a useful spin analyzer, the large TMR ratios obtained by combining Co and LSMO electrodes (50% with a STO barrier) are also an interesting result. The drawback arising from the low Curie temperature of LSMO (~350 K) is the reduction of the TMR at room temperature, down to about 5% at 300 K in Co/STO/LSMO (*4*). However, other types of oxides of the double-perovskite family (for example, $Sr_2Fe(MoO_4)$ combine electronic properties similar to those of manganites with a definitely higher Curie temperature (*15*). Their use in magnetic tunnel junctions is promising for a new generation of tunnel junctions with very high magnetoresistance for room-temperature applications.

References and Notes

1. J. S. Moodera, J. N. Nowak, R. M. Kinoy, R. Meservey, *Phys. Rev. Lett.* **74**, 3273 (1995).
2. J. De Boeck, *Science* **285**, 197 (1999).
3. M. Sharma, S. X. Wang, J. H. Nickel, *Phys. Rev. Lett.* **82**, 616 (1999).
4. J. M. De Teresa *et al.*, *ibid.*, p. 4288.
5. R. H. Tedrow and R. Meservey, *Phys. Rev. B* **7**, 318 (1973); R. Meservey and P. H. Tedrow, *Phys. Rep.* **238**, 175 (1994).
6. M. Julliere, *Phys. Lett. Magn. Magn. Mater.* **5**, 187 (1975).
7. J. A. Porto and R. Ad, *Phys. Rev. B* **9**, 3252 (1973).
8. D. Nguyen-Mahn *et al.*, *Mat. Res. Soc. Symp. Proc.* **400**, 339 (1996).
9. J. H. Park *et al.*, *Nature* **392**, 794 (1998).
10. R. Wiesendanger, H.-J. Güntherodt, G. Güntherodt, R. J. Gambino, R. Ruf, *Phys. Rev. Lett.* **65**, 247 (1990).
11. J. S. Moodera *et al.*, *ibid.*, **81**, 5553 (1998).
12. K. Wong, thesis, New York University (1999).
13. Z. Zhang, P. M. Levy, A. C. Worley, S. S. P. Parkin, *Phys. Rev. Lett.* **74**, 3644 (1995).
14. J. M. MacLaren, X.-G. Zhang, W. H. Butler, X. Wang, *Phys. Rev. B* **59**, 5470 (1999).
15. E. I. Kobayashi, Y. Ueno, H. Sawada, K. Terakura, Y. Tokura, *Nature* **395**, 677 (1998).
16. We thank A. Fert and A. Barthélémy for providing LSMO targets, R. Lyonnet and A. Vaures for their experimental help and J. Nasser for fruitful discussions. Supported by the European Union and the Human Energy and Industrial Technology Development Organization of Japan.

1 July 1999; accepted 2 September 1999

Emergence of Scaling in Random Networks

Albert-László Barabási* and Réka Albert

Systems as diverse as genetic networks or the World Wide Web are best described as networks with complex topology. A common property of many large networks is that the vertex connectivities follow a scale-free power-law distribution. This feature was found to be a consequence of two generic mechanisms: (i) networks expand continuously by the addition of new vertices, and (ii) new vertices attach preferentially to sites that are already well connected. A model based on these two ingredients reproduces the observed stationary scale-free distributions, which indicates that the development of large networks is governed by robust self-organizing phenomena that go beyond the particulars of the individual systems.

The inability of contemporary science to describe systems composed of nonidentical elements that have diverse and nonlocal interactions currently limits advances in many disciplines, ranging from molecular biology to computer science (*1*). The difficulty of describing these systems lies partly in their topology: Many of them form rather complex networks whose vertices are the elements of the system and whose edges represent the interactions between them. For example, fiv-

Department of Physics, University of Notre Dame, Notre Dame, IN 46556, USA.

*To whom correspondence should be addressed. E-mail: alb@nd.edu

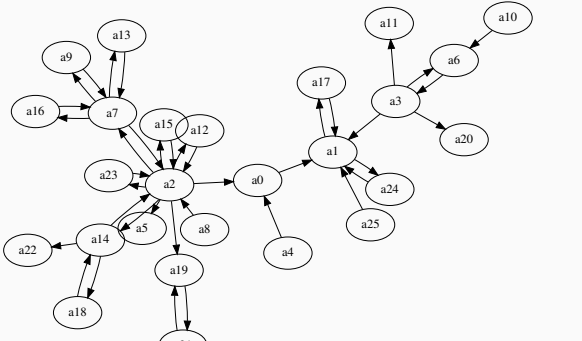

On random graphs I.

Dedicated to O. Varga, at the occasion of his 50th birthday.

By P. ERDŐS and A. RÉNYI (Budapest).

Let us consider a "random graph" $\Gamma_{n,N}$ having n possible (labelled) vertices and N edges; in other words, let us choose at random (with equal probabilities) one of the $\binom{\binom{n}{2}}{N}$ possible graphs which can be formed from the n (labelled) vertices $P_1, P_1, \ldots, P_n$ by selecting N edges from the $\binom{n}{2}$ possible edges $\overline{P_iP_j}$ $(1 \leqq i < j \leqq n)$. Thus the effective number of vertices of $\Gamma_{n,N}$ may be less than n, as some points P_i may be not connected in $\Gamma_{n,N}$ with any other point P_j; we shall call such points P_i *isolated* points. We consider the isolated points also as belonging to $\Gamma_{n,N}$. $\Gamma_{n,N}$ is called completely connected if it effectively contains all points $P_1, P_2, \ldots, P_n$ (i. e. if it has no isolated points) and is connected in the ordinary sense. In the present paper we consider asymptotic statistical properties of random graphs for $n \to +\infty$. We shall deal with the following questions:

1. What is the probability of $\Gamma_{n,N}$ being completely connected?

2. What is the probability that the greatest connected component (subgraph) of $\Gamma_{n,N}$ should have effectively $n-k$ points? $(k=0, 1, \ldots)$.

3. What is the probability that $\Gamma_{n,N}$ should consist of exactly $k+1$ connected components? $(k=0, 1, \ldots)$.

4. If the edges of a graph with n vertices are chosen successively so that after each step every edge which has not yet been chosen has the same probability to be chosen as the next, and if we continue this process until the graph becomes completely connected, what is the probability that the number of necessary steps ν will be equal to a given number l?

As (partial) answers to the above questions we prove the following four theorems. In Theorems 1, 2, and 3 we use the notation

$$N_c = \left[\frac{1}{2} n \log n + cn\right] \tag{1}$$

where c is an arbitrary fixed real number ([x] denotes the integer part of x).

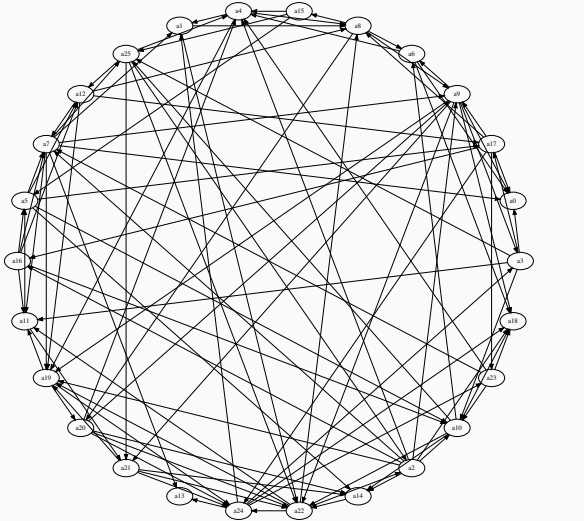

typically slower than $\sim 1\,\mathrm{km\,s^{-1}}$) might differ significantly from what is assumed by current modelling efforts[27]. The expected equation-of-state differences among small bodies (ice versus rock, for instance) presents another dimension of study; having recently adapted our code for massively parallel architectures (K. M. Olson and E.A, manuscript in preparation), we are now ready to perform a more comprehensive analysis.

The exploratory simulations presented here suggest that when a young, non-porous asteroid (if such exist) suffers extensive impact damage, the resulting fracture pattern largely defines the asteroid's response to future impacts. The stochastic nature of collisions implies that small asteroid interiors may be as diverse as their shapes and spin states. Detailed numerical simulations of impacts, using accurate shape models and rheologies, could shed light on how asteroid collisional response depends on internal configuration and shape, and hence on how planetesimals evolve. Detailed simulations are also required before one can predict the quantitative effects of nuclear explosions on Earth-crossing comets and asteroids, either for hazard mitigation[28] through disruption and deflection, or for resource exploitation[29]. Such predictions would require detailed reconnaissance concerning the composition and internal structure of the targeted object. □

Received 4 February; accepted 18 March 1998.

1. Asphaug, E. & Melosh, H. J. The Stickney impact of Phobos: A dynamical model. *Icarus* **101,** 144–164 (1993).
2. Asphaug, E. *et al*. Mechanical and geological effects of impact cratering on Ida. *Icarus* **120,** 158–184 (1996).
3. Nolan, M. C., Asphaug, E., Melosh, H. J. & Greenberg, R. Impact craters on asteroids: Does strength or gravity control their size? *Icarus* **124,** 359–371 (1996).
4. Love, S. J. & Ahrens, T. J. Catastrophic impacts on gravity dominated asteroids. *Icarus* **124,** 141–155 (1996).
5. Melosh, H. J. & Ryan, E. V. Asteroids: Shattered but not dispersed. *Icarus* **129,** 562–564 (1997).
6. Housen, K. R., Schmidt, R. M. & Holsapple, K. A. Crater ejecta scaling laws: Fundamental forms based on dimensional analysis. *J. Geophys. Res.* **88,** 2485–2499 (1983).
7. Holsapple, K. A. & Schmidt, R. M. Point source solutions and coupling parameters in cratering mechanics. *J. Geophys. Res.* **92,** 6350–6376 (1987).
8. Housen, K. R. & Holsapple, K. A. On the fragmentation of asteroids and planetary satellites. *Icarus* **84,** 226–253 (1990).
9. Benz, W. & Asphaug, E. Simulations of brittle solids using smooth particle hydrodynamics. *Comput. Phys. Commun.* **87,** 253–265 (1995).
10. Asphaug, E. *et al*. Mechanical and geological effects of impact cratering on Ida. *Icarus* **120,** 158–184 (1996).
11. Hudson, R. S. & Ostro, S. J. Shape of asteroid 4769 Castalia (1989 PB) from inversion of radar images. *Science* **263,** 940–943 (1994).
12. Ostro, S. J. *et al*. Asteroid radar astrometry. *Astron. J.* **102,** 1490–1502 (1991).
13. Ahrens, T. J. & O'Keefe, J. D. in *Impact and Explosion Cratering* (eds Roddy, D. J., Pepin, R. O. & Merrill, R. B.) 639–656 (Pergamon, New York, 1977).
14. Tillotson, J. H. Metallic equations of state for hypervelocity impact. (General Atomic Report GA-3216, San Diego, 1962).
15. Nakamura, A. & Fujiwara, A. Velocity distribution of fragments formed in a simulated collisional disruption. *Icarus* **92,** 132–146 (1991).
16. Benz, W. & Asphaug, E. Simulations of brittle solids using smooth particle hydrodynamics. *Comput. Phys. Commun.* **87,** 253–265 (1995).
17. Bottke, W. F., Nolan, M. C., Greenberg, R. & Kolvoord, R. A. Velocity distributions among colliding asteroids. *Icarus* **107,** 255–268 (1994).
18. Belton, M. J. S. *et al*. Galileo encounter with 951 Gaspra—First pictures of an asteroid. *Science* **257,** 1647–1652 (1992).
19. Belton, M. J. S. *et al*. Galileo's encounter with 243 Ida: An overview of the imaging experiment. *Icarus* **120,** 1–19 (1996).
20. Asphaug, E. & Melosh, H. J. The Stickney impact of Phobos: A dynamical model. *Icarus* **101,** 144–164 (1993).
21. Asphaug, E. *et al*. Mechanical and geological effects of impact cratering on Ida. *Icarus* **120,** 158–184 (1996).
22. Housen, K. R., Schmidt, R. M. & Holsapple, K. A. Crater ejecta scaling laws: Fundamental forms based on dimensional analysis. *J. Geophys. Res.* **88,** 2485–2499 (1983).
23. Veverka, J. *et al*. NEAR's flyby of 253 Mathilde: Images of a C asteroid. *Science* **278,** 2109–2112 (1997).
24. Asphaug, E. *et al*. Impact evolution of icy regoliths. *Lunar Planet. Sci. Conf. (Abstr.)* **XXVIII,** 63–64 (1997).
25. Love, S. G., Hörz, F. & Brownlee, D. E. Target porosity effects in impact cratering and collisional disruption. *Icarus* **105,** 216–224 (1993).
26. Fujiwara, A., Cerroni, P., Davis, D. R., Ryan, E. V. & DiMartino, M. in *Asteroids II* (eds Binzel, R. P., Gehrels, T. & Matthews, A. S.) 240–265 (Univ. Arizona Press, Tucson, 1989).
27. Davis, D. R. & Farinella, P. Collisional evolution of Edgeworth-Kuiper Belt objects. *Icarus* **125,** 50–60 (1997).
28. Ahrens, T. J. & Harris, A. W. Deflection and fragmentation of near-Earth asteroids. *Nature* **360,** 429–433 (1992).
29. *Resources of Near-Earth Space* (eds Lewis, J. S., Matthews, M. S. & Guerrieri, M. L.) (Univ. Arizona Press, Tucson, 1993).

Acknowledgements. This work was supported by NASA's Planetary Geology and Geophysics Program.

Correspondence and requests for materials should be addressed to E.A. (e-mail: asphaug@earthsci.ucsc.edu).

Collective dynamics of 'small-world' networks

Duncan J. Watts* & Steven H. Strogatz

Department of Theoretical and Applied Mechanics, Kimball Hall, Cornell University, Ithaca, New York 14853, USA

Networks of coupled dynamical systems have been used to model biological oscillators[1–4], Josephson junction arrays[5,6], excitable media[7], neural networks[8–10], spatial games[11], genetic control networks[12] and many other self-organizing systems. Ordinarily, the connection topology is assumed to be either completely regular or completely random. But many biological, technological and social networks lie somewhere between these two extremes. Here we explore simple models of networks that can be tuned through this middle ground: regular networks 'rewired' to introduce increasing amounts of disorder. We find that these systems can be highly clustered, like regular lattices, yet have small characteristic path lengths, like random graphs. We call them 'small-world' networks, by analogy with the small-world phenomenon[13,14] (popularly known as six degrees of separation[15]). The neural network of the worm *Caenorhabditis elegans*, the power grid of the western United States, and the collaboration graph of film actors are shown to be small-world networks. Models of dynamical systems with small-world coupling display enhanced signal-propagation speed, computational power, and synchronizability. In particular, infectious diseases spread more easily in small-world networks than in regular lattices.

To interpolate between regular and random networks, we consider the following random rewiring procedure (Fig. 1). Starting from a ring lattice with n vertices and k edges per vertex, we rewire each edge at random with probability p. This construction allows us to 'tune' the graph between regularity ($p = 0$) and disorder ($p = 1$), and thereby to probe the intermediate region $0 < p < 1$, about which little is known.

We quantify the structural properties of these graphs by their characteristic path length $L(p)$ and clustering coefficient $C(p)$, as defined in Fig. 2 legend. Here $L(p)$ measures the typical separation between two vertices in the graph (a global property), whereas $C(p)$ measures the cliquishness of a typical neighbourhood (a local property). The networks of interest to us have many vertices with sparse connections, but not so sparse that the graph is in danger of becoming disconnected. Specifically, we require $n \gg k \gg \ln(n) \gg 1$, where $k \gg \ln(n)$ guarantees that a random graph will be connected[16]. In this regime, we find that $L \sim n/2k \gg 1$ and $C \sim 3/4$ as $p \rightarrow 0$, while $L \approx L_{random} \sim \ln(n)/\ln(k)$ and $C \approx C_{random} \sim k/n \ll 1$ as $p \rightarrow 1$. Thus the regular lattice at $p = 0$ is a highly clustered, large world where L grows linearly with n, whereas the random network at $p = 1$ is a poorly clustered, small world where L grows only logarithmically with n. These limiting cases might lead one to suspect that large C is always associated with large L, and small C with small L.

On the contrary, Fig. 2 reveals that there is a broad interval of p over which $L(p)$ is almost as small as L_{random} yet $C(p) \gg C_{random}$. These small-world networks result from the immediate drop in $L(p)$ caused by the introduction of a few long-range edges. Such 'short cuts' connect vertices that would otherwise be much farther apart than L_{random}. For small p, each short cut has a highly nonlinear effect on L, contracting the distance not just between the pair of vertices that it connects, but between their immediate neighbourhoods, neighbourhoods of neighbourhoods and so on. By contrast, an edge

* Present address: Paul F. Lazarsfeld Center for the Social Sciences, Columbia University, 812 SIPA Building, 420 W118 St, New York, New York 10027, USA.

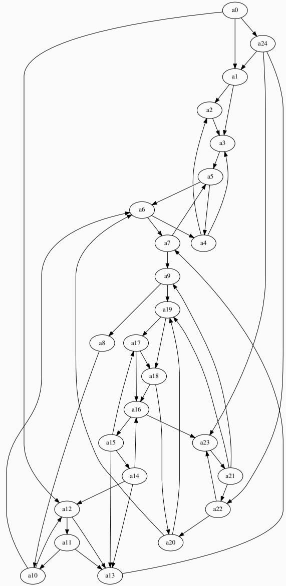

$$\text{PAR10}(s, P) = \begin{cases} 10 * T & \text{if P is unsolved} \\ t_P(s) & \text{otherwise} \end{cases}$$

T indicates the considered timeout
$t_P(s)$ denotes the time needed by solver s to solve problem P

$$\mathrm{IPC}(s, P) = \begin{cases} 0 & \text{if P is unsolved} \\ \dfrac{1}{1 + \log_{10}\left(\frac{T_P(s)}{T_P^*}\right)} & \text{otherwise} \end{cases}$$

$t_P(s)$ denotes the time needed by solver s to solve problem P
T_P^* is the minimum amount of time required by any solver to solve P

2 5 0 5 8 5 9 5 9 5 1 5 1 5
6 4 6 4 6 4 6 4 6 4 6 4 6 4
7 3 7 3 7 3 7 3 7 3 7 3 7 3
8 2 8 2 8 2 8 2 8 2 8 2 8 2

Set	Configuration	IPC Score	PAR10	Fastest (%)
Barabasi-Albert	Default	78.0	1921.0	2.5
	Configured	**125.2**	**1863.1**	**60.5**
Erdös-Rényi	Default	56.8	3426.5	16.5
	Configured	**60.4**	**3329.2**	**18.0**
Watts-Strogatz	Default	116.6	**1967.3**	**28.0**
	Configured	**118.1**	1967.9	23.5
General	Default	110.0	1665.4	11.0
	Configured	**143.0**	**1376.8**	**62.5**

Training sets	Test sets			
	Barabasi-Albert	Erdös-Rényi	Watts-Strogatz	General
Barabasi-Albert	**119.2**	6.9	34.5	42.8
Erdös-Rényi	92.3	**58.6**	105.3	125.7
Watts-Strogatz	116.2	52.6	**115.6**	129.2
General	87.5	57.6	113.5	**133.2**

Set	1st	2nd	3rd
Barabasi-Albert	S-ExtEnc (011111)	G-firstReduceDB (1528)	G-cla-decay (0.32)
Erdös-Rényi	F-autoFirst (-1.00)	G-rnd-freq (0.00)	G-K (0.26)
Watts-Strogatz	S-ExtEnc (101010)	G-Grow (0)	G-rnd-freq (0.08)
General	S-ExtEnc (101010)	G-R (2.09)	G-cla-decay (0.99)

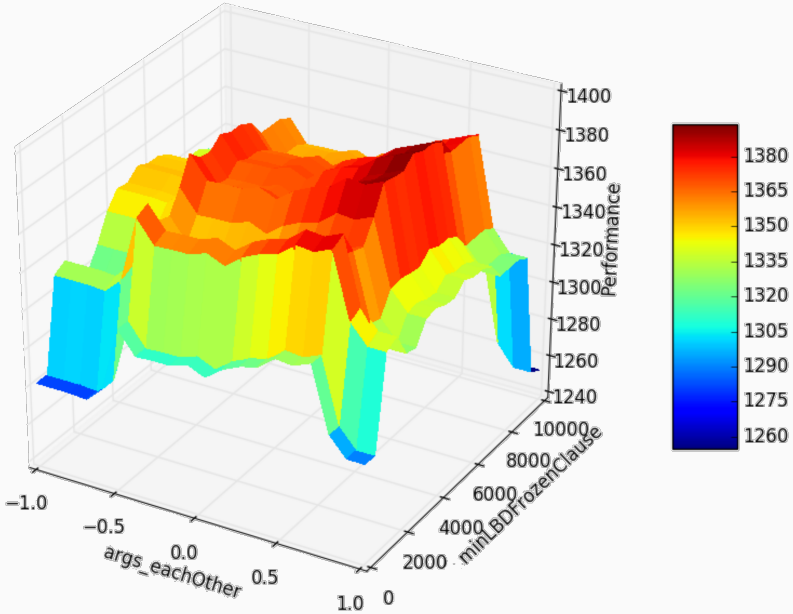
1400
1380
1360
1340
1320
1300
1280
1260
1240
Performance
1380
1365
1350
1335
1320
1305
1290
1275
1260
10000
8000
6000
4000
2000
0
minLBDFrozenClause
−1.0
−0.5
0.0
0.5
1.0
args_eachOther

CONCLUSIONS

1. We demonstrate that joint AF-solver configuration has a statistically significant impact on the performance of ArgSemSAT;

2. We demonstrate the synergies between AFs configuration and SAT solvers behaviour;

3. We open new, exciting possibilities in the area of learning for improving performance of abstract argumentation solvers.

- Evaluate the proposed joint AF-solver configuration approach on different solvers and on different problems and on different semantics;
- Exploiting the configuration approach for combining different argumentation and SAT solvers into portfolios;
- Investigating the presence of AF configurations that are able to improve—on average—the performance of all the existing state-of-the-art argumentation solvers.


CARDIFF
UNIVERSITY
PRIFYSGOL
CAERDYDD